Drug Delivery

http://informahealthcare.com/drd
ISSN: 1071-7544 (print), 1521-0464 (electronic)

Drug Deliv, 2014; 21(8): 595–604
 DOI: 10.3109/10717544.2013.865816

informa
healthcare

ORIGINAL ARTICLE

Synthesis of zirconia/polyethylene glycol hybrid materials by sol–gel processing and connections between structure and release kinetic of indomethacin

M. Catauro[1], F. Bollino[1], F. Papale[1], S. Pacifico[2], S. Galasso[2], C. Ferrara[3], and P. Mustarelli[3]

[1]*Department of Industrial and Information Engineering, Second University of Naples, Aversa, Italy,* [2]*Department of Environmental, Biological and Pharmaceutical Sciences and Technologies, Second University of Naples, Caserta, Italy, and* [3]*Department of Chemistry, Section of Physical Chemistry, University of Pavia and INSTM, Pavia, Italy*

Abstract

Controlled and local drug delivery systems of anti-inflammatory agents are attracting an increasing attention because of their extended therapeutic effect and reduced side effects. In this work, the sol–gel process was used to synthesize zirconia/polyethylene glycol (ZrO_2/PEG) hybrid materials containing indomethacin for controlled drug delivery. Different percentages of PEG were introduced in the synthesis to modulate the release kinetic and an exhaustive chemical characterization of all samples was performed to detect the relationship between their structure and release ability. Fourier transform spectroscopy and solid-state NMR show that the Zr–OH groups of the inorganic matrix bond both the ethereal oxygen atoms of the polymer and the carboxylic groups of the drug. X-ray diffraction analysis ascertains the amorphous nature of those materials. Scanning electron microscopy detects the nanostructure and the homogeneous morphology of the synthesized materials.

The bioactivity was demonstrated by the formation of a hydroxyapatite layer on the surface of the samples, after soaking in a simulated body fluid. The release kinetics study, performed by HPLC UV–Vis spectroscopy, proves that the release ability depends on PEG and the drug amount and also demonstrates the indomethacin integrity after the synthetic treatment.

Keywords

Bioactivity, drug delivery, organic/inorganic hybrid, sol–gel, solid state NMR

History

Received 16 October 2013
Revised 8 November 2013
Accepted 11 November 2013

Introduction

The class of the organic/inorganic nanocomposites hybrid materials is attracting a considerable attention today because of their properties, which come from the synergic effects of the two components and cannot be achieved otherwise, as they result from the interplay between the two phases on a nanometric scale.

Such hybrids appear promising for several applications, including the making of solid-state lasers (optical components), the use as replacements for silicon dioxide as insulating materials in the microelectronic industry, or as anticorrosion or scratch resistant coatings and host materials for chemical sensors (Dubois et al., 2008; Wang et al., 2010, 2011; Zheng et al., 2011). Also, the biomedical and pharmaceutical researches are showing a growing interest toward that class of materials. Many works suggest the use of those materials in biomedical applications (Vallet-Regi et al., 2011; Shirosaki et al., 2012; Pandey & Mishra, 2013), such as the scaffold for tissue engineering (Russo et al., 2010; Terzaki et al., 2013; De Santis et al., 2013), as biosensors (Lu & Lin, 2011), as coating to improve the biological performance of implants (Catauro et al., 2013a), or as drug delivery systems (Goldberg & Gomez-Orellana, 2003; Catauro et al., 2007a, 2008; Catauro & Bollino, 2012; Chen et al., 2013; Coll et al., 2013; Kolodziejek et al., 2013). The development of that last issue is one of the major objectives of the pharmaceutical research in order to sustain or control the release of active agents.

Controlled and localized drug release offers several advantages, if compared to other delivery options. Plasma concentrations of drugs administered via injection, inhalation, or ingestion can require repeated and relatively greater dosing, because the drug distribution occurs in whole body. The pharmacokinetics of oral drug delivery, the most popular and favorite route of administration, is influenced by some physiological and pathological factors of the patient, which can make the active principle ineffective or even toxic (Goldberg & Gomez-Orellana, 2003). Controlled local release systems may provide the desired constant drug concentrations at the delivery site, lower systemic drug levels, and a potential reduction of deleterious side effects (Danhof et al., 2008).

In this work, zirconia/polyethylene glycol (ZrO_2/PEG) hybrid materials containing indomethacin (IND) have been proposed as controlled drug delivery systems. The components choice is related to previous researches. Indeed, the use

Address for correspondence: M. Catauro, Department of Industrial and Information Engineering, Second University of Naples, Aversa, Italy. Tel: +39 0815010360. Fax: 39 0815010204. Email: michelina.catauro@unina2.it

of ceramic materials as carriers for drug release has been extensively reported in many biomedical applications (Catauro et al., 2006; Teoli et al., 2006; Habraken et al., 2007; Catauro et al., 2013b) because of their biocompatibility, mechanical, and chemical stability. The biological properties and the release ability of ZrO_2 glass systems together with the capability of same polymers, i.e. poly(ε-caprolactone) and poly(ether-imide), to modulate their release kinetic was already evaluated elsewhere by Catauro et al. (2007a,b, 2008) and Catauro & Bollino (2012).

The materials were prepared by means of the sol–gel process, a technique to make glasses and ceramics at low temperature. That method is an interesting approach to prepare hybrid materials, because it takes place in a solution, thus allowing to introduce easily the organic phases in an inorganic material, while preventing its degradation. The base reactions of sol–gel process are the hydrolysis of alkoxide precursors to form a solution (sol phase) and the condensation of the intermediate species that causes the formation of a 3D network (gel phase) (Brinker & Scherer, 1989; Hench & West, 1990).

The sol–gel process provides a convenient way to produce porous (Lu & Lin, 2011), biocompatible, and bioactive materials. The last property, that is the ability of forming an uniform apatite layer on the surface of a biomaterial allowing its strong bonding to bone *in vivo* (Kokubo et al., 2003; Catauro et al., 2007a), is related to the formation of hydroxyl groups in the inorganic network and is required to use those materials in dental and orthopedic fields.

The aim of this work is to synthesize a new class of hybrid materials for drug delivery and to investigate the release kinetic of the anti-inflammatory by the systems. A particular attention has been devoted to study the effect of the PEG on the drug release modulation and to detect the relationship of the structure and ability of those materials to release the anti-inflammatory agent. Moreover, the structural identity of the released indomethacin has been confirmed.

For that purpose, various percentages of polymer (from 0 to 50 wt%) and indomethacin (from 5 to 15%$_{wt}$) were added to the inorganic part (ZrO_2) to synthesize different hybrid systems. Their extensive chemical characterization allowed to detect a dependence between the formation of interactions among the phases and their concentration in the systems, which is responsible of a different behavior in terms of drug release.

Finally, the bioactivity of the synthesized samples has been studied by soaking them in a simulated body fluid (SBF) to evaluate their possible use in dental or orthopedic fields. In fact, the use of implantable therapeutic systems, filling materials for bone or tooth repair, which can also release pharmaceuticals (i.e. anti-inflammatory agents or antibiotics) may reduce inflammatory or infectious side effects of implant materials.

Materials and methods

Sol–gel synthesis

The organic/inorganic hybrid materials, consisting of an inorganic ZrO_2 matrix, in which different percentages of PEG (0, 6, 12, 24 and 50%$_{wt}$) were added, were synthesized by means of the sol–gel process from an analytical reagent grade of zirconium propoxide $Zr(OC_3H_7)_4$ (Sigma-Aldrich, St. Louis, MO), ethanol, water, and acetylacetone (AcAc, Sigma Aldrich, St. Louis, MO) with a molar ratio $Zr(OC_3H_7)_4$:H_2O:AcAc = 1:1:4.5. Acetylacetone was added to control the hydrolytic activity of zirconium alkoxide. Successively, PEG (PEG 400, Sigma Aldrich, St. Louis, MO), previously dissolved in ethanol, was added to the solution under vigorous stirring. ZrO_2/PEG hybrids were then all mixed with a solution of EtOH/indomethacin (5, 10 and 15 wt%) (Sigma-Aldrich, St. Louis, MO). After the addition of each reactant, the solution was stirred up to the point, by which homogeneous and transparent sols are obtained. After gelation, the gels were air-dried at 50 °C for 24 h to remove the residual solvent without any degradation of the polymer and the drug. The product obtained after that the treatment is shown in Figure 1. The flow chart in Figure 2 describes schematically the sol–gel synthesis of the said hybrid materials.

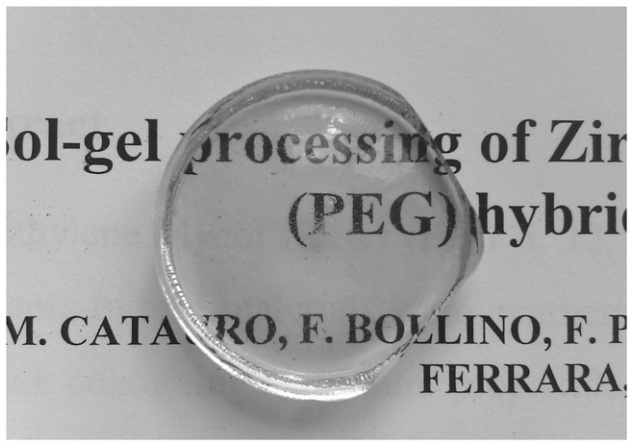

Figure 1. Bulk of ZrO_2/PEG/IND. Only one case is shown as all systems show same aspect.

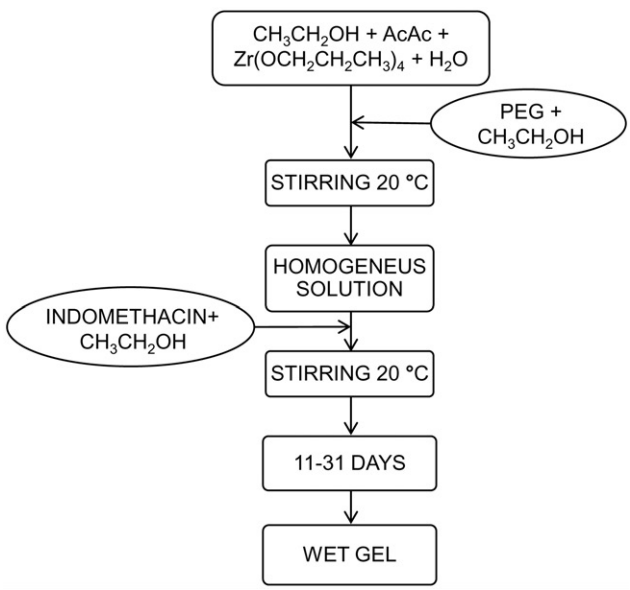

Figure 2. Flow chart of ZrO_2/PEG/IND gel synthesis.

Chemical characterization

Fourier transform infrared (FTIR) transmittance spectra were recorded in the 400–4000 cm^{-1} region using a Shimadzu Prestige 21 spectrometer, equipped with a DTGS KBr (deuterated tryglycine sulphate with potassium bromide windows) detector, with a 2 cm^{-1} resolution (45 scans). KBr pelletised disks, containing a mixture of the samples and KBr with a concentration of 1 wt%, were made and FTIR spectra were elaborated by IRsolution software (Shimadzu, Kyoto, Japan).

^{1}H–^{13}C CPMAS NMR spectra were obtained on a 400 MHz spectrometer (Avance III, Bruker) equipped with a 4 mm MAS probe. The spectra were obtained by spinning the sample at 11 kHz, with a ^{1}H 90° pulse of 3.5 µs, with a delay time of 4 s, and a contact time of 3 ms. The spectra were referenced to tetramethylsilane (TMS) and analyzed with the Topspin package (Bruker, Billerica, MA).

The nature of ZrO_2 gel and ZrO_2/PEG/IND hybrid materials was investigated by X-ray diffraction (XRD) analysis using a Philips diffractometer. Powder samples were scanned from $2\Theta = 5°$ to 60° using Cu Kα radiation.

The microstructure of the synthesized gels was studied by scanning electron microscopy (SEM, FEI Quanta 200). Before the analysis, the samples were mounted on stubs with colloidal graphite and metalized with Au.

Study of *in vitro* bioactivity

To investigate their bioactivity, the hybrids materials were soaked in a SBF with an ion concentrations almost equal to that of the blood plasma, as scheduled by Kokubo & Takadama (2006). During the soaking, the temperature was held at 37 °C. Taking into account that the ratio between the exposed surface area of the sample (S_a) and the volume of solution (V_s) influences the test, a constant ratio $S_a/V_s = 10\ mm^2\ ml^{-1}$ was used (Kokubo & Takadama, 2006).

After 21 d of incubation, the samples were rinsed in distilled water and were observed. SEM (Quanta 200) equipped with an energy dispersion spectroscopy (EDS) has been used to study the morphology of precipitate on the surface of the samples and to perform a qualitative elemental analysis.

Study of *in vitro* release

For the drug release study, discs with a 13-mm diameter and 2-mm thick were obtained by pressing 200 mg of fine gel powders (<125µm) into a cylindrical holder by means of a Specac hydraulic press.

The discs were soaked in 3.5 ml Dulbecco's phosphate buffer saline (DPBS) SBF fluid at 37 °C under continuous stirring. Drug release measurements were carried out by means of HPLC UV–Vis ESI MS analysis.

Chromatographic analyses were carried out on an Agilent 1100 HPLC system (Agilent Technologies Inc., Santa Clara, CA), equipped with a quaternary pump, a microvacuum degasser, an autosampler, a thermostatic column compartment, and a UV–Vis detector. Chromatographic separation was achieved by a Hydro® C18-reversed phase column (4 µm particle size, 150 mm × 2.0 mm i.d., Phenomenex, Torrance, CA) at a flow rate of 0.40 ml/min with isocratic elution of 0.1% (v/v) formic acid aqueous solution and acetonitrile (85:15, v/v). The UV detection of indomethacin was performed at 320 nm. To generate the calibration curve, several known concentrations of the standard (0–2.0 mM) were injected; the response factors based on the linear regression of a plot of the peak area versus the concentration were computed.

The injection volume was 10 µl. The LC system was coupled to an Api2000 QTrap (Applied Biosystem, Carlsbad, CA) with an ESI source operating in the negative mode with the following parameters: HV voltage 4500 V, dry gas N_2, 10.00 l/min with a dry temperature set at 365 °C; nebuliser 35 psi. Full-scan mass spectra of the HPLC eluates were recorded during the chromatographic separation yielding $[M-H]^-$ ions. To obtain further structural information, these ions were trapped and fragmented to yield the precursor product patterns of the analytes. The mass range was recorded from 50 to 800 *m/z*. The instruments were controlled by an Analyst Software version 1.6 (AB Sciex, MA). Drug release curves (release versus time) were normalized to the indomethacin curve by multiplying the original data by the indomethacin factor ($A_{indomethacin t=0}/A_{sample t=0}$).

Results and discussion

Sol–gel syntesis

Gelation is the result of hydrolysis and condensation reactions according to the following reactions:

$$Zr(OC_3H_7)_4 + nH_2O \Rightarrow Zr(OC_3H_7)_{4-n}(OH)_n + nC_3H_7OH \quad (1)$$

$$-ZrOH + C_3H_7O - Zr \Rightarrow \equiv Zr - O - Zr \equiv + C_3H_7OH \quad (2)$$

$$\equiv Zr - OH + OH - Zr \Rightarrow \equiv Zr - O - Zr \equiv + H_2O \quad (3)$$

The reaction mechanism is generally accepted to proceed through a second-order nucleophic substitution (Sanchez et al., 1988; Brinker & Scherer, 1989). The gelation times of the synthesized systems change as a function of the polymer and drug amounts, as shown in Table 1.

Hybrids characterization

The structure and the microstructure of the ZrO_2/PEG/IND hybrid materials were studied using FT-IR, solid-state NMR, XRD, and SEM. In Figure 3, pure indomethacin FT-IR spectrum (curve e) is compared with ZrO_2 (curve a) and ZrO_2 + IND (5, 10, and 15 wt%) (curves from b to d) gels spectra. The dominating feature of the indomethacin spectrum (curve e) is the presence of strong bands at 1710 and 1690 cm^{-1}, which can be ascribed to the vibrations of carboxylic and amide groups, respectively (Del Arco et al.,

Table 1. Gelation time in function of indomethacin and PEG amounts.

	% PEG in ZrO_2 network				
% IND in ZrO_2 network	0% PEG	6% PEG	12% PEG	24% PEG	50% PEG
5% IND	11 d	13 d	16 d	17 d	18 d
10% IND	14 d	17 d	26 d	27 d	29 d
15% IND	18 d	27 d	28 d	28 d	31 d

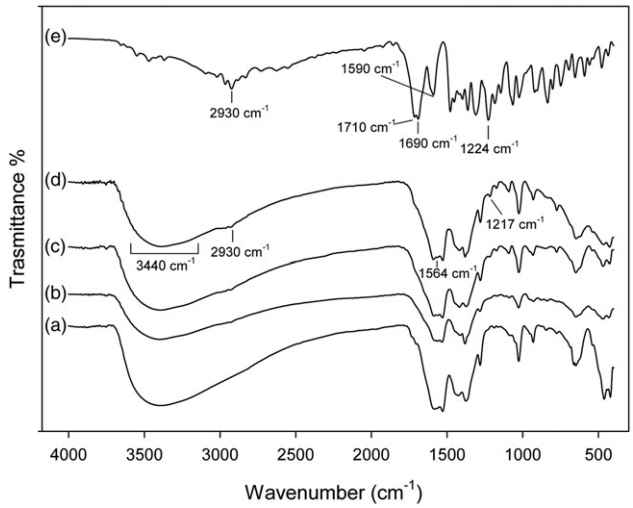

Figure 3. FT-IR spectra of (a) ZrO_2, (b–d) ZrO_2 + IND (5, 10, and 15 wt%) gels, and (e) pure indomethacin (curve e).

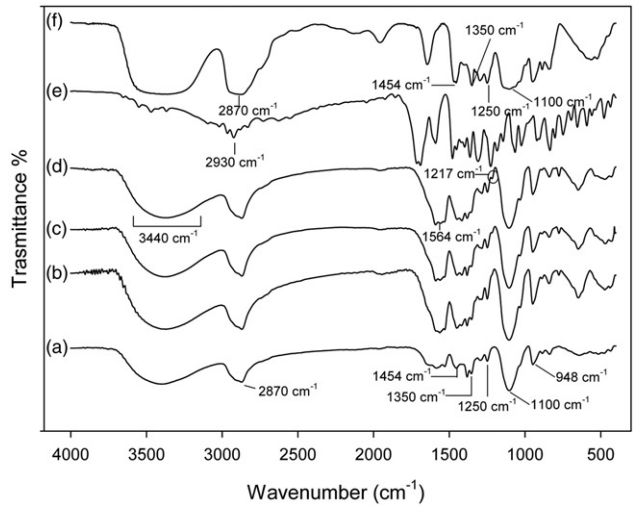

Figure 4. FT-IR spectra of (a) ZrO_2 + PEG 50 wt%$_t$, (b–d) ZrO_2 + PEG 50 wt% + IND (5, 10, and 15 wt%) gels, (e) pure indomethacin, and (f) PEG.

2004; Castro et al., 2012). Those signals, typical of the indomethacin polymorphic γ-form (Taylor & Zografi, 1997; Castro et al., 2012), disappear in ZrO_2 + IND (5, 10, and 15 wt%) spectra (Figure 3, curves b–d). A possible explanation can be found in the formation of the H-bonds between the C=O groups of the drug and the ZrO_2 inorganic matrix, which causes the lowering of the absorption frequency (Coates, 2000), whereby the indomethacin signals are covered by characteristic strong bands of ZrO_2 localized in the 1600–1400 cm^{-1} region (Georgieva et al., 2012) (Figure 3, curve a). The concurrent change in the shape of the broad band attributed to –OH vibrations at 3440 cm^{-1}, which can be observed by comparing curve a with b, c, and d, supports such hypothesis. In the ZrO_2 + IND (5, 10, and 15 wt%) systems spectra (Figure 3, curves b–d), however, some peaks are visible (i.e. those at 2930 cm^{-1} due to methyl ($–CH_3$) vibration) whose intensities increase with the drug amount, thus confirming the presence of indomethacin in those materials (Coates, 2000). Moreover, the bands that are present in the indomethacin spectrum (Figure 3 curve e) at 1590 cm^{-1}, assigned to –C–C– stretching of the aromatic rings, and at 1224 cm^{-1}, due to –C–O– stretching of ether group (Del Arco et al., 2004), appear to be shifted to 1564 and 1217 cm^{-1}, respectively, in the hybrid systems spectra (Figure 3 curves b–d). That evidence suggests the establishment of weak interactions between the drug and the ZrO_2 matrix, which perturb the delocalization of the aromatic ring electrons (Coates, 2000). The said peaks are also present in the spectra of all the systems containing both the drug and the polymer, as shown in Figure 4 where, as an example, PEG and indomethacin spectra (curves f and e) are compared with ZrO_2 + 50% PEG + IND (0%, 5%, 10%, 15%) spectra (curves from a to d). In those spectra the typical peaks of PEG are also present. The intensity of those last peaks increase with the polymer amount, as it is evident in Figure 5, where the PEG spectrum (curve f) is compared with those of the hybrid systems containing 15%$_{wt}$ IND and different amounts of PEG (0 to 50 wt%) (curves from a to e). The typical PEG methylene C–H stretching band at 2870 cm^{-1} appears in curve b and its intensity increases (from b to e) together

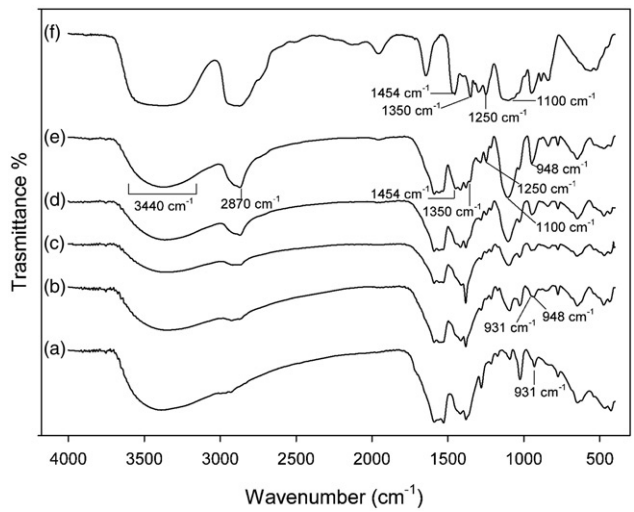

Figure 5. FT-IR spectra of (a) ZrO_2 + IND 15 wt%, (b–e) ZrO_2 + PEG (6, 12, 24, and 50 wt%) + IND 15 wt% gels, and (f) PEG.

with methylene C–H bending of the polymer at 1454 cm^{-1} (Coates, 2000). Also, the peaks due to alcohols C–O and ethereal C–O–C stretching at 1250 and 1100 cm^{-1}, respectively (Coates, 2000), appear to be increasing from b to e. Moreover, the sharp AcAc C–C–H bend, typical of the ZrO_2 spectrum (Figure 5, curve a) at 931 cm^{-1} (Gallo & Piccirillo, 2012; Georgieva et al., 2012) is replaced with a little broader peak at 948 cm^{-1} attributed to PEG C–C stretching (Coates, 2000). Finally, the change in the shape of the broad band at 3440 cm^{-1} suggests the formation of hydrogen bonds, which is also probably occur between the –OH groups of the inorganic matrix and the ethereal oxygen atoms of the PEG chains (H-bond donors).

Solid-state NMR confirms the FTIR results. Figure 6 shows the ^{13}C–^{1}H CPMAS spectrum of pure indomethacin (curve b) compared with that of ZrO_2 + IND 15 wt% (curve a). Indomethacin exists in two possible polymorphs, e.g. α (meta-stable) and γ (stable) (Masuda et al., 2006; Gallo & Piccirillo, 2009). The spectrum of Figure 6, in excellent

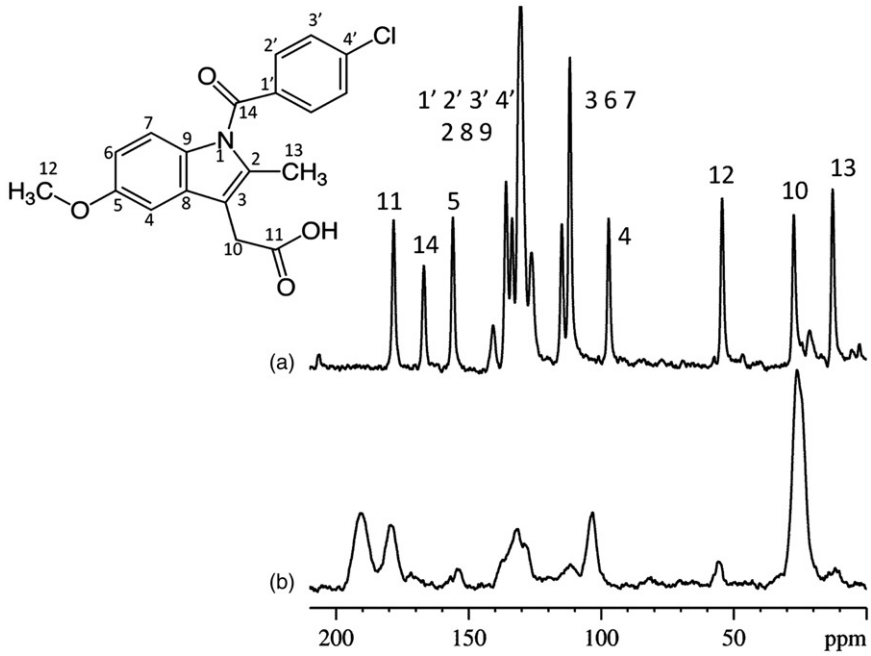

Figure 6. ^{13}CPMAS NMR spectra of (a) pure indomethacin and (b) ZrO_2 + IND 15 wt%.

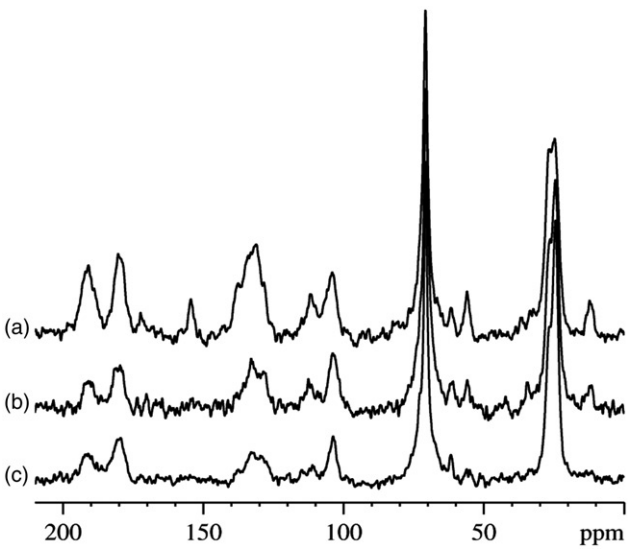

Figure 7. ^{13}C–^{1}H CPMAS spectra of (a–c) ZrO_2 + 12 wt% PEG + IND (5, 10, and 15 wt%).

agreement with that reported by Masuda et al. (2006), clearly points to the γ moiety. The peaks assignment is reported in Figure 7 following the determinations of Masuda et al. We refer to that paper for further details. The presence of the inorganic part causes: (i) a generalized increase of the peaks linewidth due to disorder, (ii) a variation of the peaks intensity, probably due to different magnetization transfers during CP contact time, (iii) relevant shift downfield (10 and 15 ppm, respectively) of the carbons 11 and 14, which is in agreement with the formation of a hydrogen bonds scheme, and (iv) a modification of the spectral features of the aromatic ring bonded to the ether oxygen. This last result is not easy to explain and requires some specific DFT calculations to be addressed.

Figure 7 shows, as an example, the ^{13}C–^{1}H CPMAS spectra of ZrO_2 + PEG 12 wt% with the addition of different amounts of indomethacin (from 5 to 15 wt%) (curves from a to c). The corresponding spectra with 24 and 50 wt% of PEG are similar. No significant differences are observed among the spectra. The characteristic peaks of PEG400 may be clearly observed at 71 ppm (C–O chain carbons), and 62 ppm (C–OH terminal carbons) (Domján et al., 2009). The peaks are very large due to intrinsic disorder. The addition of indomethacin does not induce any significant change in the position and shape of peaks, besides the increase of a peak at about 155 ppm when passing from 5% to 15% of the drug. This peak is due to the carbon (5) of indomethacin (see Figure 6a). We also stress here that CP-MAS is not a quantitative technique because of possibly unequal magnetization transfer from protons to carbons.

Figure 8 shows the ^{13}C–^{1}H CPMAS spectra of ZrO_2 + IND 15 wt% with the addition of different amounts of PEG (from 0 to 50 wt%) (curves from a to e). The addition of the polymer does not determine relevant changes in the indomethacin peaks, but for small changes of the peak shape of the aliphatic carbon 10, which was already reported to be structured (Masuda et al., 2006). A shoulder at about 73 ppm is observed in the main PEG peak, which can be probably attributed to a non-covalent interaction among a small fraction of the ether oxygens with the carboxyl group of the indomethacin molecule. Interestingly, this interaction is confirmed by the aliphatic carbon 10 (see inset B) rather than by the carboxyl 11. However, the combined analysis of Figures 7 and 8 shows that there are no strong interactions among the indomethacin molecules and the polymer strands.

Those observations allow to classify the synthesized materials as class I hybrids (hybrids characterized by weak bonds between the two phases), according to Judenstein et al.'s classification (Judeinstein & Sanchez, 1996).

Figure 9 shows the diffractograms of indomethacin (panel a) and ZrO_2 + PEG 50 wt% + IND 15 wt% (panel b). In pure indomethacin diffractogram crystallinity peaks are clearly visible, which disappear completely in the

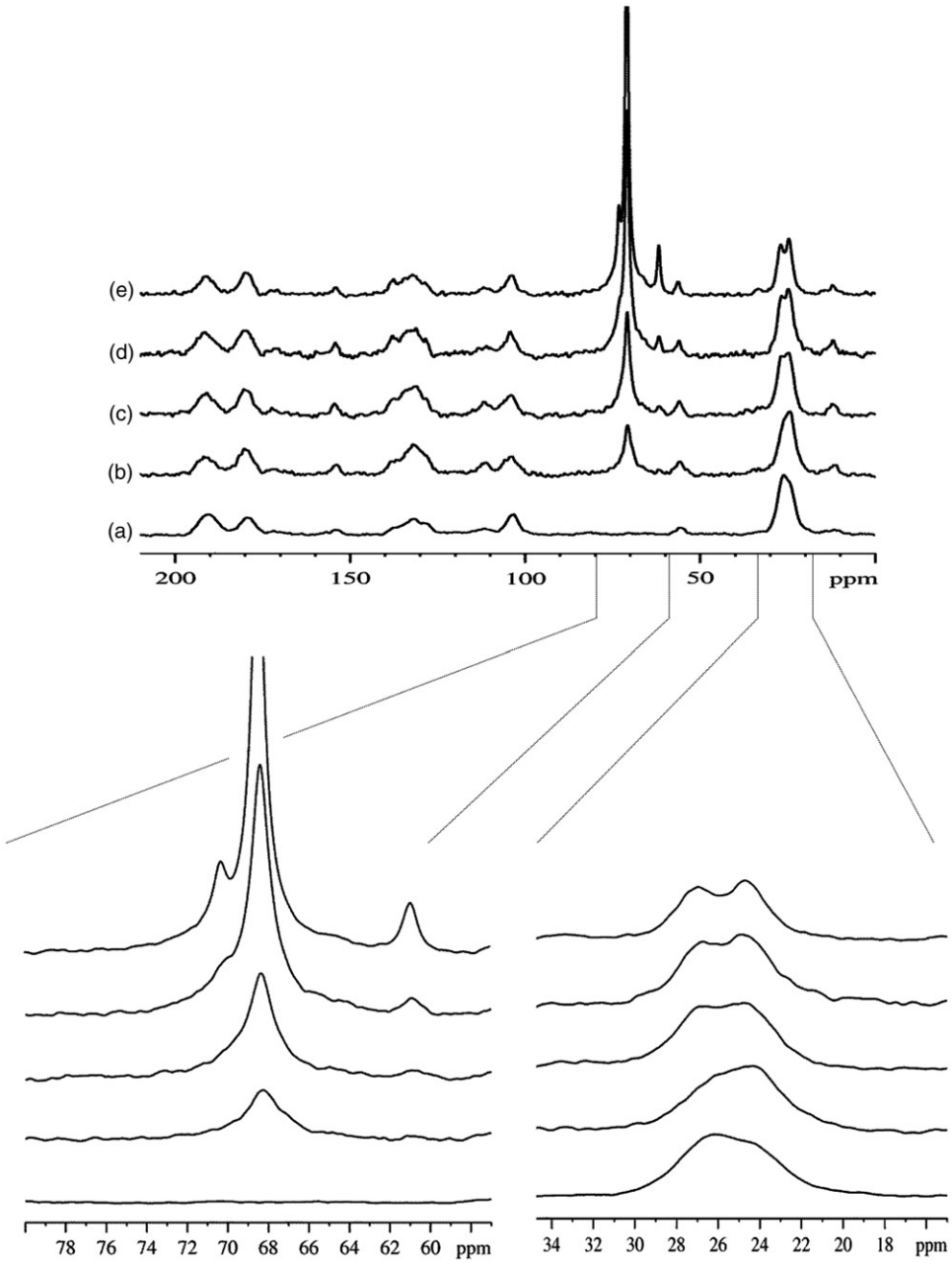

Figure 8. ^{13}C–^{1}H CPMAS spectra of (a) ZrO_2 + IND 15 wt% and (b–e) ZrO_2 + PEG (6, 12, 24, and 50 wt%) + IND 15 wt%.

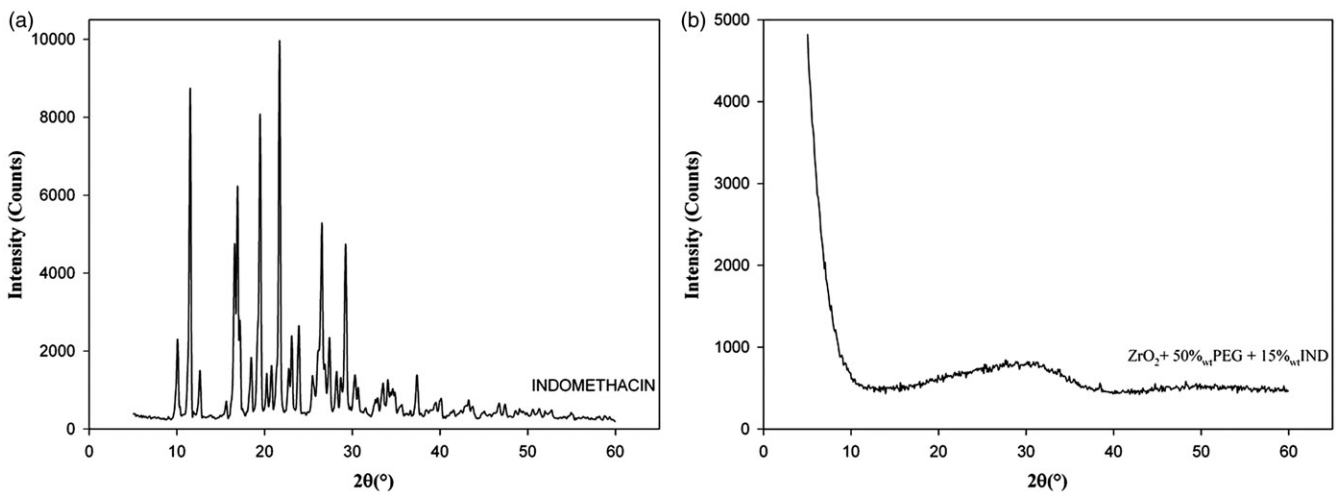

Figure 9. XRD spectra of (a) pure indomethacin and (b) ZrO_2 + 50% PEG + IND 15 wt%.

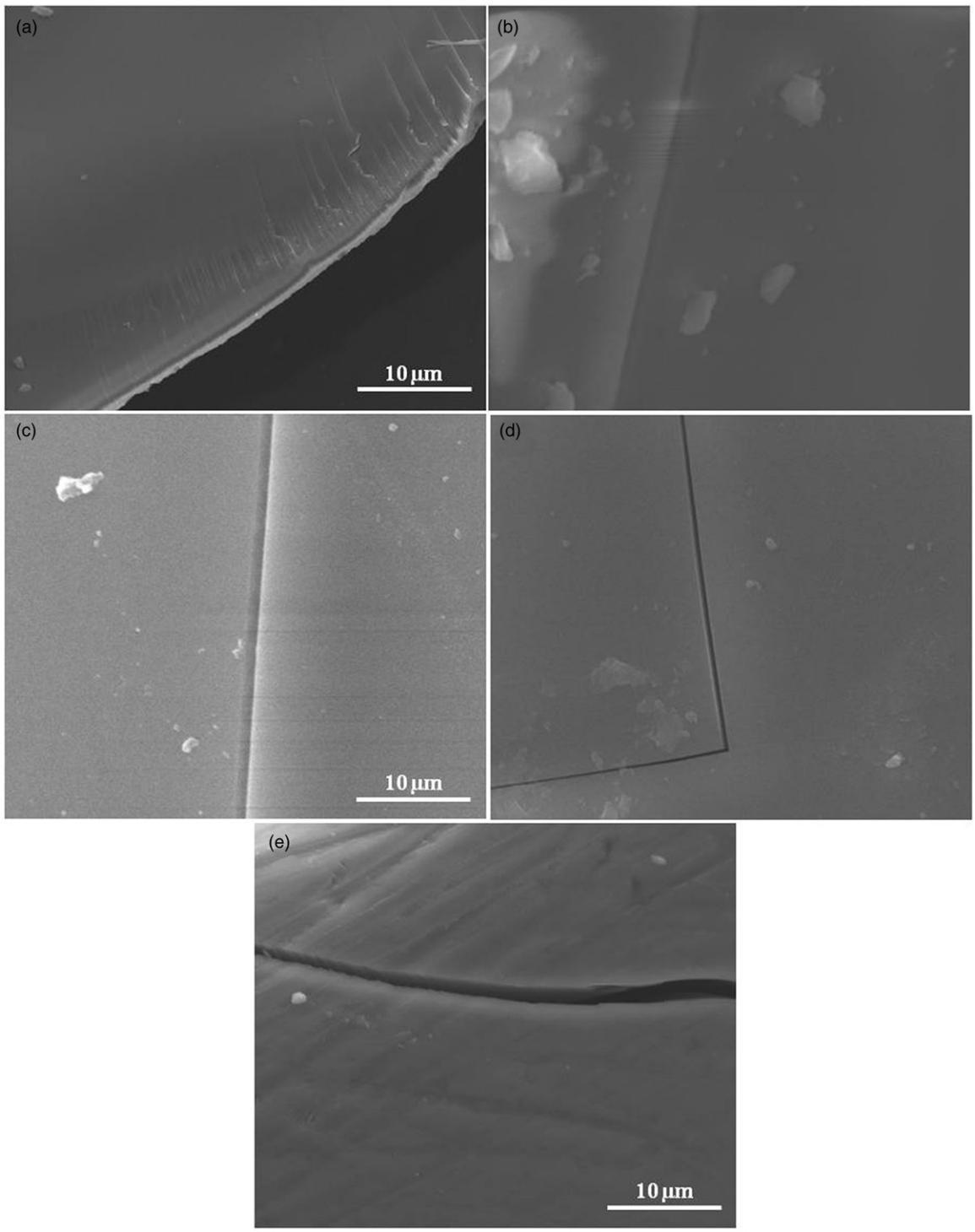

Figure 10. SEM micrograph of (a) ZrO_2 (b–e) ZrO_2 + PEG (6, 12, 24, and 50 wt%) + IND 15 wt%.

diffractogram of the hybrid materials. All samples exhibit the characteristics broad humps of amorphous materials, for this reason only a diffractogram is shown as an example (see Figure 9b).

The surfaces of all synthesized systems were observed by SEM and no significant differences were noted. Figure 10 shows the SEM micrographs of ZrO_2 (panel a) and hybrid systems containing different amounts of PEG (from 6 to 50 wt%) and 15 wt% of indomethacin (panels from b to e). All systems appear to be homogeneous and no separation of phases is visible even at high magnifications, thus confirming that the synthesized materials are nanostructured hybrid ones.

Bioactivity and EDS analysis

SEM micrographs of the hybrid materials after soaking in SBF for 21 d (Figure 11a) show the characteristic apatite globular crystals on the surface of all systems with a similar distribution. The confirmation that the surface layer observed in the SEM micrographs is composed of calcium phosphate is given by EDS analyses, reported in Figure 11(b).

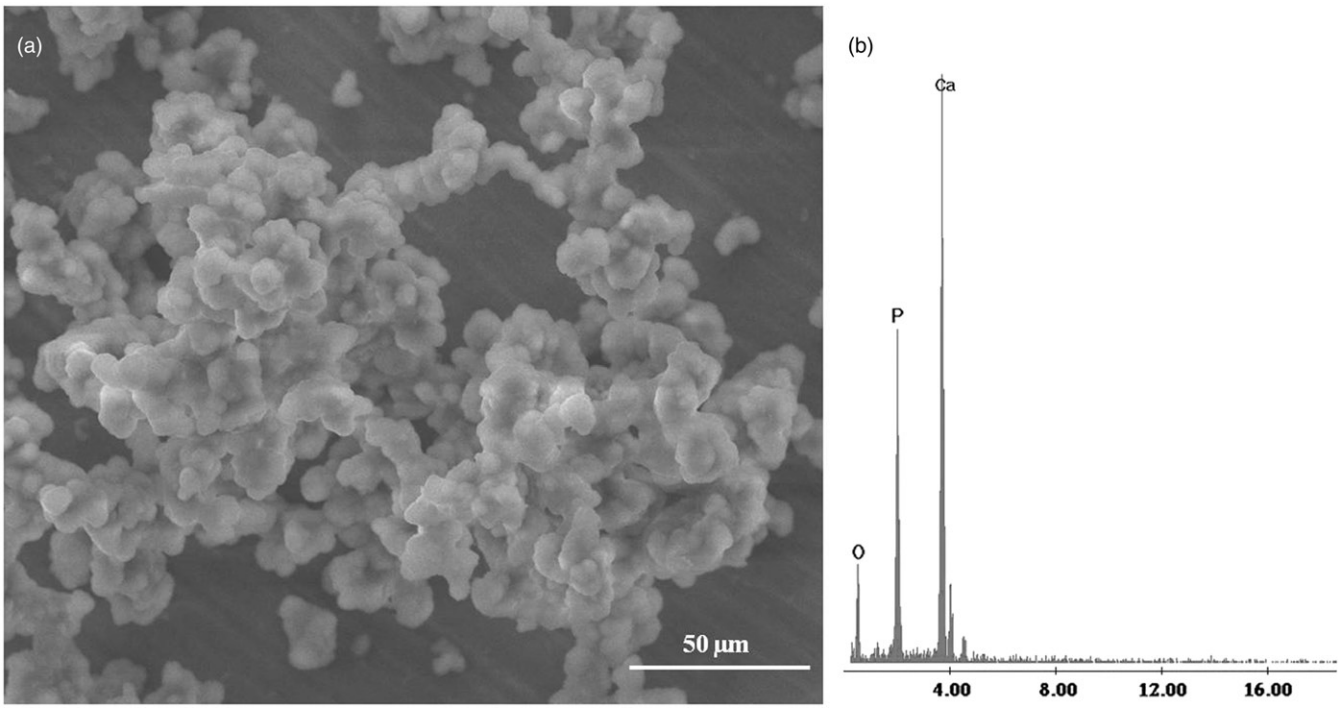

Figure 11. SEM micrograph of a sample surface after bioactivity test. (a) Hydroxyapatite globular crystals and (b) EDS elementary analyses of crystals.

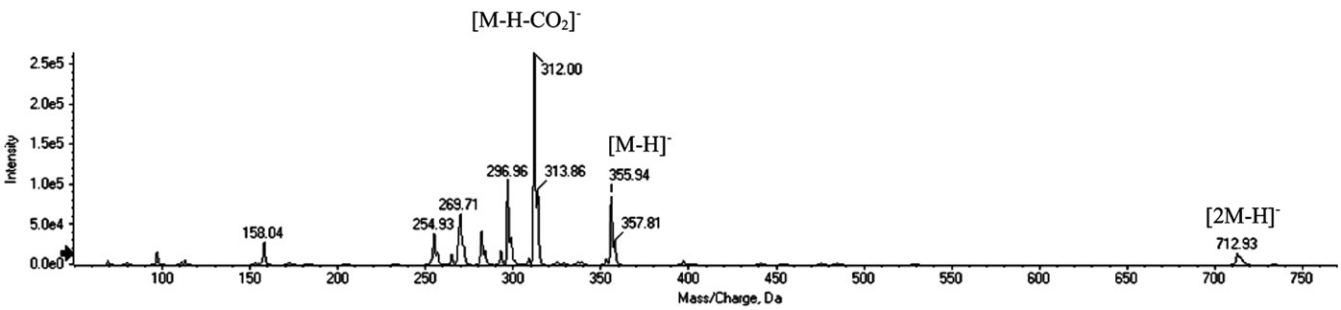

Figure 12. Indomethacin ESI(−)-MS spectrum.

The ratio between the atomic content of Ca and P is 1.6, in agreement with the chemical formula of hydroxyapatite (Uchida et al., 2001).

The formation of apatite on the materials may be caused due to the presence of Zr–OH groups on their surface. These groups could lose protons and increase the negative charge on the surface, thus attracting the calcium ion (Wu et al., 2013). These ions combine with the negative charge of the phosphate ions to form the amorphous phosphate, which spontaneously transforms into hydroxyapatite $[Ca_{10}(PO_4)_6(OH)_2]$ (Hench, 1991; Li et al., 2013).

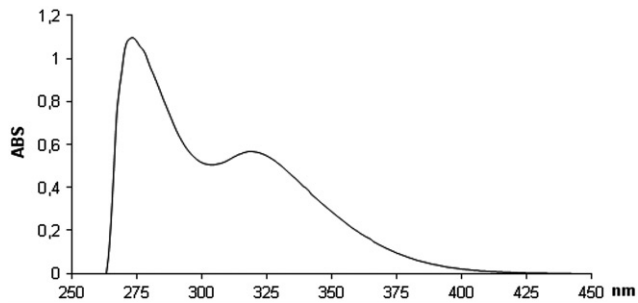

Figure 13. Indomethacin (30 µM) UV spectrum in DPBS.

Release kinetics

Kinetic measurements of indomethacin release were performed through HPLC coupled with UV and ESI-MS detectors. Indomethacin was quantitatively determined by HPLC-UV, and LC–MS was used to direct its identification (Figure 12).

Calibration curves were prepared plotting UV and MS peaks area versus drug concentrations (0–2.0 mM). Both the calibration curves showed an excellent linearity within the tested range. Although indomethacin has two absorbance peaks in the UV region (Figure 13), HPLC-UV analysis was carried out at 320 nm as zirconium propoxide exhibited absorption starting at around 270 nm. From all the discs, previously transferred in phosphate buffered saline, the samples were collected and introduced into HPLC apparatus, daily, for 25 d thereafter. The analysis time was chosen on the basis of the behavior of the samples containing only zirconium propoxide and indomethacin at the three considered

w/w percentages. Within the tested indomethacin doses, there was a rough exponential increase of its release in the saline solution. Figure 14 shows that indomethacin release from materials not containing PEG reached a plateau at 13–17 d. The concentration of indomethacin and its interactions with the inorganic matrix seem to play a role in the release kinetics. In fact, it has been observed that the discs with the lowest dose of the drug could promote a faster release than that from discs with 10 and 15 wt% of indomethacin.

The introduction of the polymer (Figure 15) modulates the drug release differently. Discs with a 6 wt% PEG percentage show an increased release rate, which is independent from the indomethacin concentration, with significant data from as early as day 10. When the system ZrO_2 + PEG 12 wt% was analyzed, it was observed that a similar behavior for discs containing 5 wt% of indomethacin; the release from ZrO_2 + PEG 12 wt% +IND 10 and 15 wt% was slower. PEG percentages equal to 24 and 50 wt% do not seem to determine a full release of the drug.

This is probably due to the formation of a polymeric network capable of trapping anti-inflammatory molecules, probably through the weak interactions (detected by NMR) between the drug and PEG, which start when the polymer is added in high amounts and make difficult the full availability of indomethacin.

The spectrometric time-dependent analysis of eluates confirms the structural identity of the drug, thus suggesting the ability of the adopted method of synthesis to preserve the pharmacological properties of indomethacin.

Conclusions

The sol–gel process has allowed to synthesize organic/inorganic hybrid materials consisting of a ZrO_2 inorganic matrix, in which different percentages of a polymer (PEG) and an ant-inflammatory agent (IND) were entrapped. Their amorphous and nanostructured nature was ascertained by means of XRD and SEM analyses, respectively.

FTIR and solid-state NMR detected that the inorganic matrix makes H-bonds with both PEG ethereal oxygen atoms and carboxylic groups of indomethacin (H-bond acceptors) by means of –OH groups (H-bond donators). The bonds strength is a function of the amounts of both the polymer and the drug and affects the ability of the synthesized systems to release the anti-inflammatory. It has been observed that systems containing a lower dose of indomethacin release faster independently from the polymer amount. Moreover, PEG presence increases the release rate independently from the drug concentration, but that effect is countered when the polymer percentages are high (24 and 50 wt%). In the last case, a full release of drug does not occur, probably because of the formation of weak interactions between indomethacin and PEG which start when the polymer is added in high amounts (as suggest by NMR) and make difficult the full availability of the drug. LC-MS analysis confirms the structural identity of the drug released by hybrid materials, which hence should preserve its pharmacological activity.

Finally, the formation of a hydroxyapatite layer on the ZrO_2/PEG/IND samples surface after soaking in SBF indicates that the synthesized systems can be considered bioactive materials.

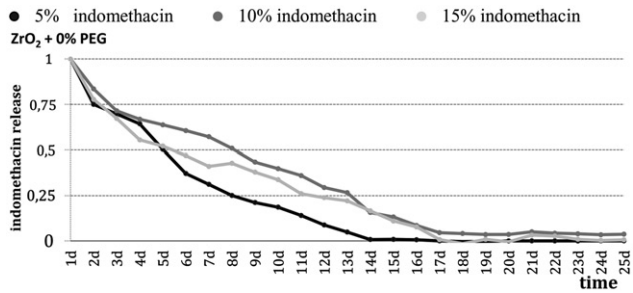

Figure 14. Time-dependent indomethacin release plot for the ZrO_2 + IND (5, 10, and 15 wt%) systems.

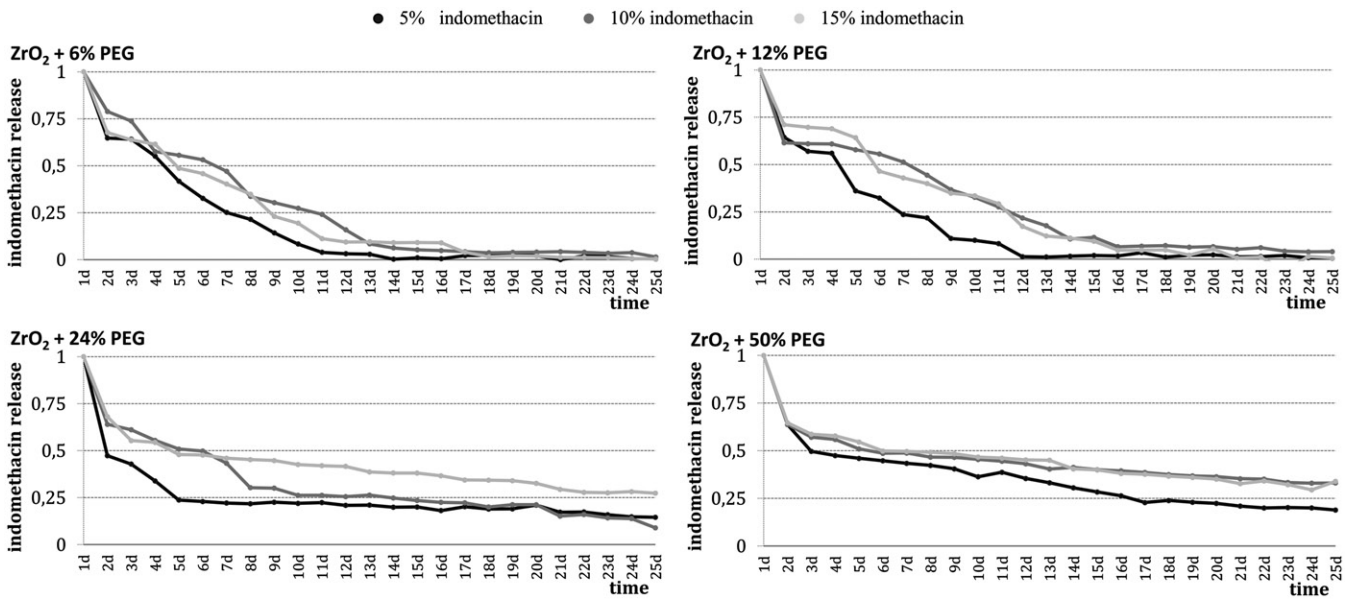

Figure 15. Time-dependent indomethacin release plot for the ZrO_2 + PEG (6, 12, 24, and 50 wt%) + IND (5, 10, and 15 wt%) systems.

In conclusion, the obtained data allow us to hypothesize the successful use of the prepared hybrid materials as modified-release systems, in which the speed and duration of the release of the active ingredient can be modulated and hence programmed.

Declaration of interest

The authors report no declarations of interest.

Reference

Brinker C, Scherer G. (1989). Sol–gel science: the physics and chemistry of sol–gel processing. San Diego: Academic Press.

Castro SG, Ramirez-Rigo MV, Allemandi, DA, Palma SD. (2012). New binary solid dispersion of indomethacin and croscarmellose sodium: physical characterization and *in vitro* dissolution enhancement. J Excipients Food Chem 3:121–8.

Catauro M, Bollino F. 2012. Anti-inflammatory entrapment in polycaprolactone/silica hybrid material prepared by sol–gel route, characterization, bioactivity and in vitro release behavior. J Appl Biomater Funct Mater. doi: 10.5301/JABFM.2012.9256.

Catauro M, Bollino F, Papale F. (2013a). Preparation, characterization and biological properties of organic–inorganic nanocomposite coatings on titanium substrates prepared by sol–gel. J Biomed Mater Res A. doi: 10.1002/jbm.a.34721.

Catauro M, Bollino F, Papale F. (2013b). Synthesis of SiO_2 system via sol gel process: biocompatibility tests with a fibroblast strain and release kinetics. J Biomed Mater Res A. doi: 10.1002/jbm.a.34836.

Catauro M, Raucci M, Ausanio G. (2008). Sol–gel processing of drug delivery zirconia/polycaprolactone hybrid materials. J Mater Sci: Mater Med 19:531–40.

Catauro M, Raucci MG, Ausanio C, Ambrosio L. (2007a). Sol–gel synthesis, characterization and bioactivity of poly(ether-imide)/TiO_2 hybrid materials. J Appl Biomater Biomech 5:41–8.

Catauro M, Raucci MG, Continenza MA. (2007b). Release kinetics of ampicillin, biocompatibility tests with a fibroblast strain of a zirconia gel glass. Lett Drug Des Discov 4:453–9.

Catauro M, Raucci MG, Convertito C, et al. (2006). Characterization, bioactivity and ampicillin release kinetics of TiO_2 and $TiO_2 4SiO_2$ synthesized by sol–gel processing. J Mater Sci: Mater Med 17: 413–20.

Chen Z, Li Z, Lin Y, et al. (2013). Biomineralization inspired surface engineering of nanocarriers for pH-responsive, targeted drug delivery. Biomaterials 34:1364–71.

Coates, J. (2000). Interpretation of infrared spectra, a practical approach. In: Meyers RA, ed. Encyclopedia of analytical chemistry. Chichester: John Wiley & Sons Ltd., 10815–37.

Coll C, Bernardos A, Martinez-Manez R, Sancenon F. (2013). Gated silica mesoporous supports for controlled release and signaling applications. Acc Chem Res 46:339–49.

Danhof M, De Lange ECM, Della Pasqua OE, et al. (2008). Mechanism-based pharmacokinetic-pharmacodynamic (PK-PD) modeling in translational drug research. Trends Pharmacol Sci 29:186–91.

De Santis R, Gloria A, Russo T, et al. (2013). Advanced composites for hard-tissue engineering based on PCL/organic–inorganic hybrid fillers: from the design of 2D substrates to 3D rapid prototyped scaffolds. Polym Compos 34:1413–17.

Del Arco M, Cebadera E, Gutiérrez, S, et al. (2004). Mg, Al layered double hydroxides with intercalated indomethacin: synthesis, characterization, and pharmacological study. J Pharmaceut Sci 93:1649–58.

Domján A, BAJDIK, J, Pintye-Hódi K. (2009). Understanding of the plasticizing effects of glycerol and PEG 400 on chitosan films using solid-state NMR spectroscopy. Macromolecules 42:4667–73.

Dubois G, Volksen W, Magbitang T, et al. (2008). Superior mechanical properties of dense and porous organic/inorganic hybrid thin films. J Sol–gel Sci Technol 48:187–93.

Gallo A, Piccirillo AM. (2009). On some generalizations Bellman–Bihari result for integro-functional inequalities for discontinuous functions and their applications. Boundary Value Probl. doi:10.1155/2009/808124.

Gallo A, Piccirillo AM. (2012). Multidimensional impulse inequalities and general bihari type inequalities for discontinuous functions with delay. Nonlinear Stud 19:115–26.

Georgieva I, Danchova N, Gutzov S, Trendafilova N. (2012). DFT modeling, UV–Vis and IR spectroscopic study of acetylacetone-modified zirconia sol–gel materials. J Mol Model 18:2409–22.

Goldberg M, Gomez-Orellana I. (2003). Challenges for the oral delivery of macromolecules. Nat Rev Drug Discov 2:289–95.

Habraken WJEM, Wolke JGC, Jansen JA. (2007). Ceramic composites as matrices and scaffolds for drug delivery in tissue engineering. Adv Drug Deliv Rev 59:234–48.

Hench LL. (1991). Bioceramics: from concept to clinic. J Am Ceram Soc 74:1487–510.

Hench LL, West JK. (1990). The sol–gel process. Chem Rev 90:33–72.

Judeinstein P, Sanchez C. (1996). Hybrid organic–inorganic materials: a land of multidisciplinarity. J Mater Chem 6:511–25.

Kokubo T, Kim H-M, Kawashita M. (2003). Novel bioactive materials with different mechanical properties. Biomaterials 24:2161–75.

Kokubo T, Takadama H. (2006). How useful is SBF in predicting in vivo bone bioactivity? Biomaterials 27:2907–15.

Kolodziejek J, Glowka E, Hyla K, et al. (2013). Relationship between surface properties determined by inverse gas chromatography and ibuprofen release from hybrid materials based on fumed silica. Int J Pharm 441:441–8.

Li J, Yang J, Li J, et al. (2013). Bioinspired intrafibrillar mineralization of human dentine by PAMAM dendrimer. Biomaterials 34: 6738–47.

Lu B, Lin YS. (2011). Sol–gel synthesis and characterization of mesoporous yttria-stabilized zirconia membranes with graded pore structure. J Mater Sci 46:7056–66.

Masuda K, Tabata S, Kono H, et al. (2006). Solid-state 13C NMR study of indomethacin polymorphism. Int J Pharmaceut 318:146–53.

Pandey S, Mishra SB. (2013). Bioceramics: silica-based organic–inorganic hybrid materials for medical applications. Hoboken, NJ: John Wiley & Sons, Inc., 135–61.

Russo T, Gloria A, D'Antò V, et al. (2010). Poly(ε-caprolactone) reinforced with sol–gel synthesized organic-inorganic hybrid fillers as composite substrates for tissue engineering. J Appl Biomater Biomech 8:146–52.

Sanchez C, Livage J, Henry M, Babonneau F. (1988). Chemical modification of alkoxide precursors. J Non-Crystalline Solids 100: 65–76.

Shirosaki Y, Osaka A, Tsuru K, Hayakawa S. (2012). Inorganic–organic sol–gel hybrids. Chichester, UK: John Wiley & Sons Ltd., 139–58, 1 plate.

Taylor LS, Zografi G. (1997). Spectroscopic characterization of interactions between PVP and indomethacin in amorphous molecular dispersions. Pharm Res 14:1691–8.

Teoli D, Parisi L, Realdon N, et al. (2006). Wet sol–gel derived silica for controlled release of proteins. J Control Release 116:295–303.

Terzaki K, Kissamitaki M, Skarmoutsou A, et al. (2013). Pre-osteoblastic cell response on three-dimensional, organic–inorganic hybrid material scaffolds for bone tissue engineering. J Biomed Mater Res A 101:2283–94.

Uchida M, Kim HM, Kokubo T, et al. (2001). Bonelike apatite formation induced on zirconia gel in a simulated body fluid and its modified solutions. J Am Ceram Soc 84:2041–4.

Vallet-Regi M, Colilla M, Gonzalez B. (2011). Medical applications of organic-inorganic hybrid materials within the field of silica-based bioceramics. Chem Soc Rev 40:596–607.

Wang H, Akid R, Gobara M. (2010). Scratch-resistant anticorrosion sol–gel coating for the protection of AZ31 magnesium alloy via a low temperature sol–gel route. Corros Sci 52:2565–70.

Wang S, Zhao L, Sun J, et al. (2011). Preparation of stable second-order nonlinear optical films by sol–gel technique. Polym Adv Technol 22: 759–62.

Wu D, Yang J, Li J, et al. (2013). Hydroxyapatite-anchored dendrimer for *in situ* remineralization of human tooth enamel. Biomaterials 34: 5036–47.

Zheng Y, Tan C, Wang Q, Zhang CC. (2011). 2-(3-Pyridyl)imidazole-4,5-dicarboxylic acid based lanthanide luminescent anion sensor. Solid State Sci 13:1687–91.